Light-Induced Self-Poling Effect on Organometal Trihalide Perovskite Solar Cells for Increased Device Efficiency and Stability

*Yehao Deng, Zhengguo Xiao, and Jinsong Huang**

Organolead trihalide perovskites (OTPs) are a family of organic–inorganic hybrid semiconductors that are promising for low-cost solar cells.[1,2] The power conversion efficiency (PCE) of OTP solar cells has increased with an unprecedented growth rate from 3.8% in 2009[3] to over 20% in late 2014.[4] The high PCE has been attributed to long carrier diffusion length,[5–8] high absorption coefficient,[9,10] nonexcitonic nature of OTP materials,[11] and other mechanisms.[12] Among all the interesting properties discovered for OTP materials and devices, a giant switchable photovoltaic effect discovered by us recently is unique in that it is only found in OTP-based devices, and could potentially impact the device stability of the OTP-based electronic devices.[13] The field switchable photovoltaic effect was found to be caused by the migration/drift of charged ions or vacancies under applied field, e.g., $CH_3NH_3^+$ (MA^+), I vacancy ($V_I^{\cdot}$).[13,14] Recently, we observed migration of MA^+ directly using composition sensitive scanning probe microscopy in the lateral structure OTP devices.[14] The motion of those ions/vacancies may also result in current hysteresis when changing the scanning direction during current–voltage (I–V) measurement and even reverse the photocurrent direction if the electrodes are not selective.[13–18] While the impact of motion of ions/vacancies on transient response of the OTP devices is now acknowledged,[17–19] the influence of motion of ions/vacancies under electric field on longer term device stability is still unknown, although there are already speculation that it can be a potential threat to the long-term stability of the OTP devices.[18,20]

It is shown by computation and experiments that positive ions/vacancies can n-type dope while negative space charges can p-type dope the OTP materials, thus an asymmetric distribution of space charges in OTP layer may result in a p-i-n or n-i-p homojunction structure that can potentially enhance the apparent performance of OTP solar cells.[12–14,21,22] In addition, we have proven that an applied external electric field as low as 1 V μm^{-1}, corresponding to a voltage of less than 0.33 V for a 300 nm thick $MAPbI_3$ layer, can switch the photocurrent direction in a device structure of indium tin oxide (ITO)/poly(3,4-ethylenedioxythiophene):poly(styrenesulfonate) (PEDOT:PSS)/$CH_3NH_3PbI_3$ ($MAPbI_3$)/Au (50 nm).[13] We thus speculate that the photovoltage of the devices, which is generally above 0.33 V, is large enough to drive the drift of ions/vacancies in OTP devices with 300 nm thick $MAPbI_3$. In this Communication, we show that the light-generated photovoltage also causes drift of ions/vacancies in the same way as the applied external bias, and the migration of ions increases the PCE of the working OTP solar cells under illumination.

The device structure of the first studied OTP solar cell is ITO/PEDOT:PSS/$MAPbI_3$ (300 nm)/Au (50 nm), as is shown in **Figure 1**a, which has a switchable photovoltaic effect as demonstrated by us previously.[13] The as-prepared (pristine) device under 1 sun illumination (100 mW cm^{-2}) shows poor performance with small short circuit current (J_{SC}) of –10.5 mA cm^{-2}, open circuit voltage (V_{OC}) of 0.24 V, and FF (fill factor) of 13.1% (Figure 1b, blue line in region 4) because of the similar work function of PEDOT:PSS and Au. The photocurrents were scanned from 0 to 1 V at a high sweep rate of 0.31 V s^{-1} to minimize poling effect during the scanning process.[13] However, after illuminating the device at 1 sun (100 mW cm^{-2}) for 2 min, an obvious PCE increase was observed, with the J_{SC}, V_{OC}, and FF enhanced to –20.3 mA cm^{-2}, 0.5 V, and 40.0%, respectively (red line). This enhancement is reversible if we store the device in dark condition for about 2 min, after which the performance goes back to the original level (purple line). Therefore this enhancement is not caused by poling effect during scanning but by illumination indeed. We have shown previously that the polarity of the device can be switched by scanning from –2.5 V to 0 V, after which the I–V curve was flipped to region 2.[13] Here we slightly poled the device so that the photocurrent direction was just switched, named as preswitched device (Figure 1b, in region 2), while we limited the electric poling time so that the device's starting V_{OC} was around –0.2 V to observe the light-induced poling effect (blue line in region 2). Consistently, we observed that illumination improved the performance of preswitched device as well (red line in region 2). The effect of light-induced photovoltaic performance change is thus termed as "Light-Induced Self-Poling (LISP)" effect. It demonstrates that the LISP process can be triggered on only if there is a preset V_{OC} with a device nonsymmetry, and LISP increases the degree of the device nonsymmetry by increasing the band-bending.

To determine the evolution of device performance change under illumination over time, we measured V_{OC} change under 1 sun illumination for a relatively long duration, and the V_{OC}–illumination time plots for pristine and preswitched devices are shown in Figure 1c. The V_{OC} of initial pristine device was 0.12 V, but climbed rapidly up to 0.4 V in 15 s, and finally saturated at over 0.46 V with extended illumination time up to 100 s.

Y. Deng, Dr. Z. Xiao, Prof. J. Huang
Department of Mechanical and Materials Engineering
University of Nebraska-Lincoln
Lincoln, NE 68588-0656, USA
E-mail: jhuang2@unl.edu

DOI: 10.1002/aenm.201500721

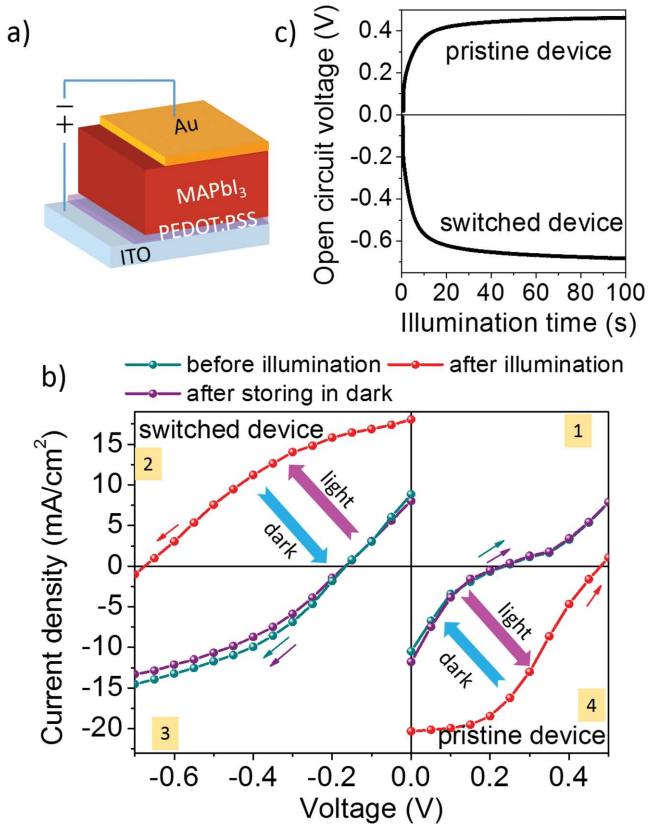

Figure 1. a) Device structure of switchable OTP solar cells. b) Current–voltage of the as-prepared (pristine) and preswitched device before illumination (blue line), after illumination (100 mW cm^{-2}) for 2 min (red line), and after storage in dark again for 2 min (purple line). The voltage was scanned from 0 V to ±1 V at a high rate of 0.31 V s^{-1}. The arrows indicate the scan direction. c) V_{OC} versus illumination time for both pristine and preswitched devices.

Similarly, the V_{OC} of preswitched device increased rapidly from –0.18 V to –0.60 V in 15 s and finally saturated at –0.68 V.

The LISP effect can be well explained by the drift of ions/vacancies in $MAPbI_3$ under the additional photovoltage added under illumination. We have shown previously that ions/vacancies in OTP layer drift under applied external electric field.[13,14] The positive ions/vacancies accumulated at one side of OTP layer to act as space charges, causing n-type doping in the local OTP material, and the remaining negative space charges can p-type dope the OTP material on the other side, forming a p-i-n or n-i-p homojunction.[12–14,21,22] The as-prepared device with symmetrical work function electrodes has limited photovoltaic performance because of the too small built-in potential. When the device is illuminated, the photovoltage acts as an additional bias applied to the device, which breaks the equilibrium state of the device established in dark and starts to pole the OTP layer. The electric field of photovoltage points from PEDOT:PSS to Au electrode, so it drives the positive ions/vacancies to drift toward Au electrode (**Figure 2**a). The accumulated space charges close to Au side enhance the n-type doping concentration in that region, which increases the band-bending and thus the built-in voltage as well as the V_{OC} of the devices (Figure 2b). The increased V_{OC} further drives the drift of ions/vacancies, which forms a positive feedback cycle. On the other hand, the back diffusion of ions/vacancies becomes strong also once there is significant accumulation of ions, which reduces the band-bending. The V_{OC} saturates when the drift and reverse diffusion of those ions/vacancies are balanced. It is noted that the work functions of both electrodes in these devices are comparable; therefore, the observed V_{OC} should be caused by the band-bending in the perovskite layer.

The preset V_{OC} direction determines the LISP direction, which explains why LISP enhances the performance of both pristine and preswitched devices (Figure 1b). In addition, there

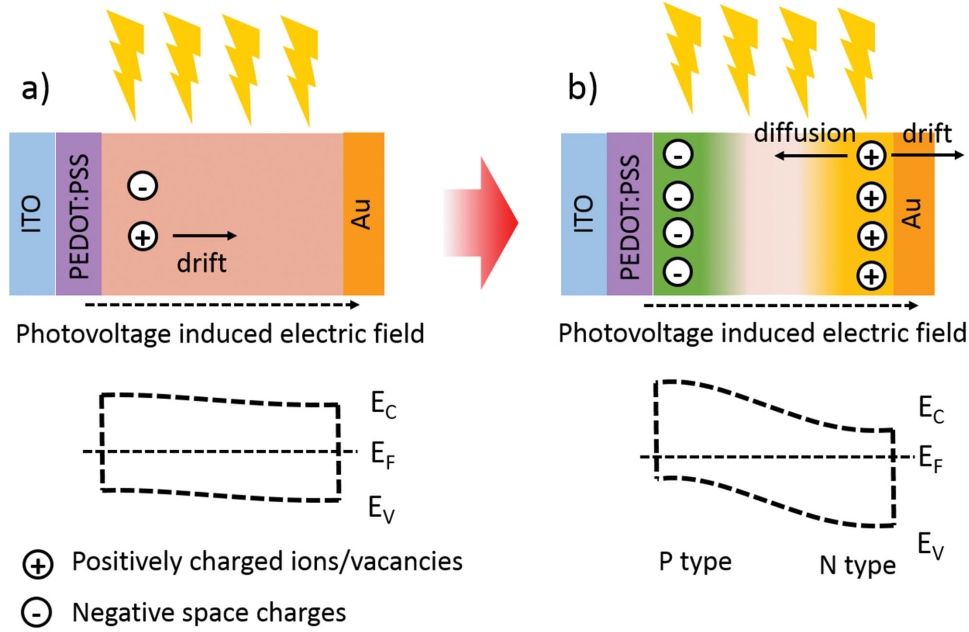

Figure 2. Schematic showing the light-induced self-poling (LISP) process in OTP solar cells and the energy diagram in OTP layer a) before and b) after LISP.

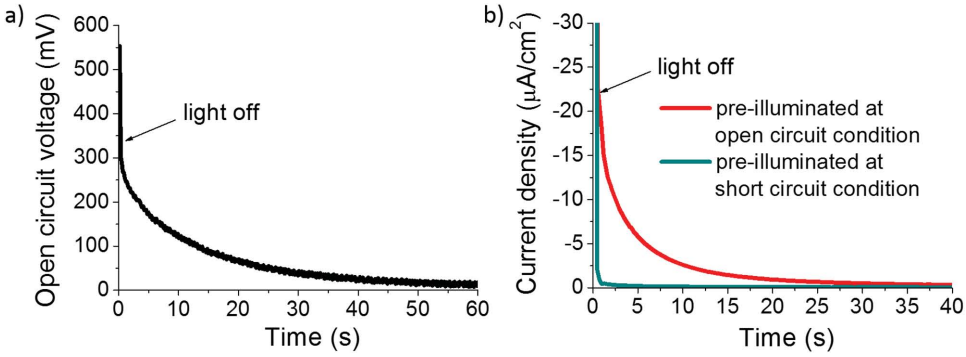

Figure 3. a) Transient open-circuit voltage in the dark after preillumination in open-circuit condition. b) Transient short-circuit current in dark condition after illumination in either open-circuit condition (red line) or short-circuit condition (blue line).

should be no difference of ions drifting inside the devices no matter whether the bias is applied externally or from the photovoltage. To verify this, we poled the pristine and preswitched devices by applying an external bias of 0.46 V and −0.68 V in the dark for about 1 min, respectively, which are close to the maximum V_{OC} of these solar cells. It was found that J–V curves after electrical poling match well with those after light poling (Figure S1, Supporting Information).

The drifted ions/vacancies by LISP process can be investigated by studying their back diffusion in the dark, when there is no ion drift driven by photovoltage, and thus only ion back diffusion occurs. The back diffusion of ions/vacancies results in nonzero transient V_{OC} and J_{SC} in the dark, whose directions are consistent with that of photovoltage and photocurrent, respectively. In **Figure 3**a, the V_{OC} decay in the dark was measured after preilluminating the device at open-circuit condition for 2 min. The initial V_{OC} in dark remained 55% of the V_{OC} under 1 sun illumination and decreased gradually in tens of seconds. The time scale is typical for ion movement.[18] Figure 3b shows the J_{SC} decay measured after illuminating the device at open-circuit condition (red line). The J_{SC} in dark was initially larger than −20 μA cm^{-2}, and gradually decreased to zero in tens of seconds. By integrating the transient current with time, and considering the geometry of the $MAPbI_3$ layer (300 nm thick and 7 mm^2 in area), the accumulated charge density in the $MAPbI_3$ layer is calculated to be 2.1×10^{19} cm^{-3} after 2 min illumination. Such high charge density is not likely to come from detrapping of trapped electrons/holes, as the trap density is usually on the order of $10^{10–13}$ cm^{-3},[23] but is comparable to that obtained by electric poling induced ions movement.[16] It should be noted that the doping density is much higher than that of fresh $MAPbI_3$ film prepared in the same way,[22] indicating that the large amount of mobile ions/vacancies should be generated by light.[17,20,24] In sharp contrast, the device preilluminated in short-circuit condition has very small transient J_{SC} in the dark (<2 μA cm^{-2}) (Figure 3b, blue line). This is easy to understand because when the device is in short-circuit condition, there is no photovoltage to drive the drift of ions/vacancies.

The LISP occurs not only in device with symmetrical work function electrodes but also in regular unidirectional devices. We inserted a layer of phenyl-C61-butyric acid methyl ester (PCBM) (20 nm) between $MAPbI_3$ and Au electrode to break the electrode symmetry (inset in **Figure** 4b). PCBM acts as an electron transport material with strong charge selectivity.[25] The device is nonswitchable/unidirectional as it had decent PCE when scanned from 2.5 V to −0.5 V (Figure 4a, green line) but had negligible PCE when scanned from −2.5 V to 0.5 V (Figure 4a, black line), showing that the PCBM layer effectively blocks the hole transport and only allows unidirectional current flow. The as-prepared device before illumination has a V_{OC} of 0.66 V, J_{SC} of −17.9 mA cm^{-2}, and FF of 36.5% when scanned from 0 to 1.1 V (Figure 4a, blue line). After illumination for 2 min, the V_{OC}, J_{SC}, and FF increased to 0.98 V, −18.9 mA cm^{-2}, and 49.0%, respectively (Figure 4a, red line), approaching the performance obtained by high forward bias (2.5 V) poling (Figure 4a, green line). The V_{OC}–illumination time plot is shown in Figure 4b. The V_{OC} climbed up rapidly from 0.45 to 0.6 V in only 1 s after the 1 sun light was turned on, and then increased steadily to 1.02 V in 60 s. It should be noted that the V_{OC} of unidirectional device (0.45–1.0 V) is generally higher than that of switchable device (0.2–0.65 V), which indicates the V_{OC} of the device is not determined by the energy level of the Au electrode.[26] The J_{SC} enhancement by LISP is relatively small, though, because the exciton dissociates and charge collection efficiency is not very sensitive to the built-in field due to small exciton binding energy in $MAPbI_3$ and very long carrier diffusion length.[5,11] The transient dark current and voltage of the unidirectional device are included in Figure S2 (Supporting Information), showing the same phenomenon as that of the switchable devices.

The increased built-in potential by LISP illustrated in Figure 2 can be directly observed from the dark I–V curve of OTP solar cell before and after illumination (Figure 4c). The device before illumination does not show a typical I–V curve from a junction (blue line), while after illumination the curve shows well-developed carrier injection barrier, which is resulted from increased built-in potential (red line), as shown by the energy diagram in Figure 2b. It should be noted that the lowest current density of the red curve is not at zero bias, which is consistent with the fact that the V_{OC} is not zero in the dark right after turning off illumination. The stabilized photocurrent at the maximum power point (0.63 V) is shown in Figure 4d. It increases from near zero to 12.8 mA cm^{-2} in 500 s, corresponding to a huge PCE enhancement from zero to 8.1%.

Finally we infer that LISP is a general effect and occurs in all kinds of OTP solar cells despite they have different degree

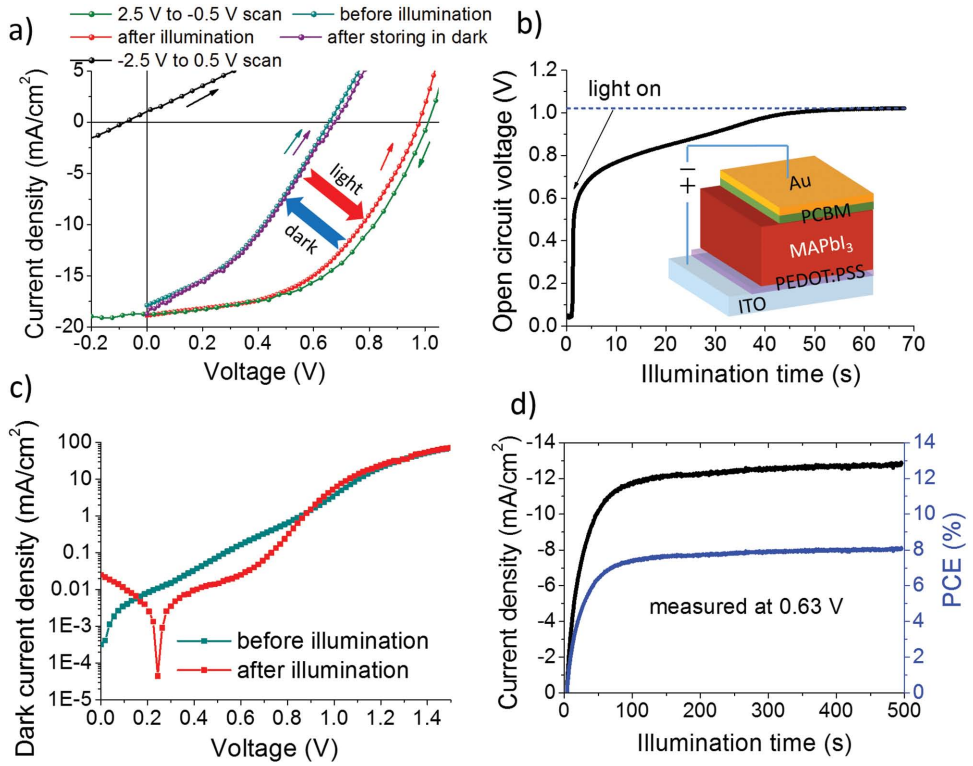

Figure 4. a) Current–voltage characteristics of as-prepared unidirectional device (blue line), which is then illuminated at 100 mW cm^{-2} for 2 min (red line) and stored in the dark for 2 min (purple line). The green and black lines are current–voltage curves by scanning from ± 2.5 V to 0 V to see if the device polarity can be switched. b) V_{OC}-illumination time plot. The unidirectional device structure is shown in the inset. c) The dark current–voltage curve of the unidirectional solar cell before and after illumination. d) Photocurrent at maximum power point (0.63 V) versus illumination time along with the calculated PCE.

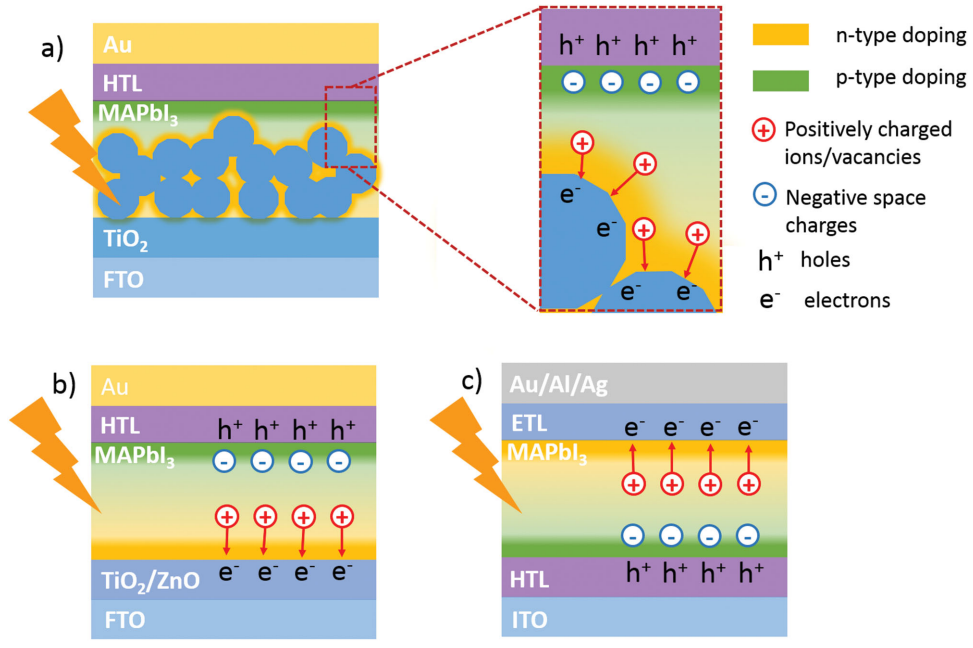

Figure 5. Device structure and light-induced self-poling process illustration for a) TiO_2-based mesoporous solar cell, b) TiO_2/ZnO-based planar solar cell, and c) organic hole/electron transportation layer (HTL/ETL) based inverted planar solar cell.

of poling effect. First of all, this effect should be anticipated in other OTP materials such as $MAPbBr_3$, $FAPbI_3$, $MAPbI_{3-x}Cl_x$, $MAPbI_{3-x}Br_x$, etc., as they have been proven to have similar migration effect as that of $MAPbI_3$.[13] Second, this light-poling effect is independent of the device structure of OTP solar cells, including TiO_2-based mesoporous solar cell **(Figure 5**a), TiO_2/ZnO-based planar solar cell (Figure 5b), and organic hole/electron transportation layer (HTL/ETL) based inverted planar solar cells (Figure 5c). No matter along what direction carriers are transporting and collected, the photovoltage shall always drive ions/vacancies drift to form a favorable p-i-n homojunction in situ that further enhances built-in potential of the devices (Figure 5a–c). Third, since those ions/vacancies migrate only within the OTP layer, it is independent of ETL/HTL and electrode materials. Indeed, it was observed that the photocurrent of OTP solar cells with different structure based on $MAPbI_3$,[27,28] $MAPbI_{3-x}Cl_x$,[15,19] or $(FAPbI_3)_{0.85}(MAPbBr_3)_{0.15}$[4] at its maximum power point increased with continued illumination if they were stored in dark before testing. Though trap-filling is also a possible origin to account for this phenomenon, the time scale of tens of seconds or longer indicates that it is more likely to be induced by ion motion.[18] In addition, the persistent V_{OC} in the dark after illumination is reported by several groups.[29,30] Though the origin is not fully understood, some possible mechanisms, such as detrapping[29] and carrier recombination process,[30] have been excluded, and ion migration should be the reasonable mechanism behind. We want to point out several reasons why the general LISP effect is often underestimated or neglected: (1) The devices maybe have been unintentionally illuminated by strong light at open-circuit condition before *I–V* testing. (2) The LISP finishes quickly if perovskite films have optimum condition for fast ion drift,[31] e.g., the presence of high density of mobile ions/vacancies, large grain boundary density, and high initial photovoltage. (3) The device performance has already been optimized so that the built-in electrical field from work function difference between anode and cathode out-performs the contribution from p-i-n homojunction by LISP.

In conclusion, we showed that light illumination improved the performance of both symmetrical and unidirectional OTP solar cells significantly. Based on our previously finding on electric poling and doping principle of OTP materials, we suggest that this improvement can be explained by directional drift of ions/vacancies in OTP materials driven by photovoltage-induced electric field, forming p-i-n homojunction in situ that improves the performance of OTP solar cells. This study shows that those mobile ions/vacancies actually improve the efficiency in OTP solar cells. In addition, the spontaneous p-i-n homojunction formation by illumination should relieve the strict structure requirement, and simplify the fabrication procedure for OTP solar cells, providing additional unique properties that have not been envisioned in traditional organic or inorganic solar cells.

Experimental Section

Device Fabrication: Poly(3,4-ethylenedioxythiophene):poly(4-styrenesulfonate) (PEDOT:PSS) (Baytron-P 4083) was spin-coated at 3000 rounds per minute (rpm) on UV-ozone-treated ITO substrates for 40 s and then annealed at 130 °C in air for 20 min. After cooling down, the substrates were transferred to a nitrogen (N_2) filled glove box. PbI_2 (400 mg mL^{-1}) and MAI (50 mg mL^{-1}) dissolved in dimethylformamide at 90 °C and 2-propanol, respectively, were spin-coated on to substrates sequentially at 6000 rpm for 35 s, followed by thermal annealing at 100 °C for 30 min. After that, the devices were finished by thermal evaporation of 50 nm gold (Au) as electrode. For device with a layer of 20 nm PCBM in between $MAPbI_3$ and Au, PCBM dissolved in dichlorobenzene at 20 mg mL^{-1} was spin-coated on $MAPbI_3$ layer at 6000 rpm for 35 s, followed by thermal annealing at 100 °C for 10 min before the thermal evaporation of Au electrode.

Device Characterization: The AM 1.5G irradiation (100 mW cm^{-2}) was simulated by a Xenon-lamp-based solar simulator (Oriel 67005, 150 W Solar Simulator). A Schott visible-color glass-filtered (KG5 color-filtered) Si diode (Hamamatsu S1133) was used to calibrate the light intensity before photocurrent measurement. A Keithley 2400 source-meter was used to apply scanning bias and test the output current simultaneously. All the electrical tests were conducted in glove box.

Supporting Information

Supporting Information is available from the Wiley Online Library or from the author.

Acknowledgements

This work was financially supported by the National Science Foundation under Awards ECCS-1252623 and DMR-1420645.

Received: April 12, 2015
Revised: July 2, 2015
Published online: August 7, 2015

[1] M. A. Green, A. Ho-Baillie, H. J. Snaith, *Nat. Photon.* **2014**, *8*, 506.
[2] H. S. Jung, N. G. Park, *Small* **2015**, *11*, 10.
[3] A. Kojima, K. Teshima, Y. Shirai, T. Miyasaka, *J. Am. Chem. Soc.* **2009**, *131*, 6050.
[4] N. J. Jeon, J. H. Noh, W. S. Yang, Y. C. Kim, S. Ryu, J. Seo, S. I. Seok, *Nature* **2015**, *517*, 476.
[5] Q. Dong, Y. Fang, Y. Shao, P. Mulligan, J. Qiu, L. Cao, J. Huang, *Science* **2015**, *347*, 967.
[6] D. Shi, V. Adinolfi, R. Comin, M. Yuan, E. Alarousu, A. Buin, Y. Chen, S. Hoogland, A. Rothenberger, K. Katsiev, Y. Losovyj, X. Zhang, P. A. Dowben, O. F. Mohammed, E. H. Sargent, O. M. Bakr, *Science* **2015**, *347*, 519.
[7] G. Xing, N. Mathews, S. Sun, S. S. Lim, Y. M. Lam, M. Grätzel, T. C. Sum, *Science* **2013**, *342*, 344.
[8] S. D. Stranks, G. E. Eperon, G. Grancini, C. Menelaou, M. J. Alcocer, T. Leijtens, H. J. Snaith, *Science* **2013**, *342*, 341.
[9] J. H. Im, C. R. Lee, J. W. Lee, S. W. Park, N. G. Park, *Nanoscale* **2011**, *3*, 4088.
[10] H. S. Kim, C. R. Lee, J. H. Im, K. B. Lee, T. Moehl, A. Marchioro, S. J. Moon, R. Humphry-Baker, J. H. Yum, J. E. Moser, M. Gratzel, N. G. Park, *Sci. Rep.* **2012**, *2*, 591.
[11] M. Hu, C. Bi, Y. Yuan, Z. Xiao, Q. Dong, Y. Shao, J. Huang, *Small* **2015**, *11*, 2164.
[12] W.-J. Yin, T. Shi, Y. Yan, *Appl. Phys. Lett.* **2014**, *104*, 063903.
[13] Z. Xiao, Y. Yuan, Y. Shao, Q. Wang, Q. Dong, C. Bi, P. Sharma, A. Gruverman, J. Huang, *Nat. Mater.* **2015**, *14*, 193.

[14] Y. Yuan, J. Chae, Y. Shao, Q. Wang, Z. Xiao, A. Centrone, J. Huang, *Adv. Energy Mater.* **2015**, DOI: 10.1002/aenm.201500615.
[15] H. J. Snaith, A. Abate, J. M. Ball, G. E. Eperon, T. Leijtens, N. K. Noel, S. D. Stranks, J. T.-W. Wang, K. Wojciechowski, W. Zhang, *J. Phys. Chem. Lett.* **2014**, *5*, 1511.
[16] Y. Zhao, C. Liang, H. m. Zhang, D. Li, D. Tian, G. Li, x. Jing, W. Zhang, W. Xiao, Q. Liu, F. Zhang, Z. He, *Energy Environ. Sci.* **2015**, *8*, 1256.
[17] E. L. Unger, E. T. Hoke, C. D. Bailie, W. H. Nguyen, A. R. Bowring, T. Heumüller, M. G. Christoforo, M. D. McGehee, *Energy Environ. Sci.* **2014**, *7*, 3690.
[18] W. Tress, N. Marinova, T. Moehl, S. M. Zakeeruddin, M. K. Nazeeruddin, M. Grätzel, *Energy Environ. Sci.* **2015**, *8*, 995.
[19] Y. Zhang, M. Liu, G. E. Eperon, T. Leijtens, D. McMeekin, M. Saliba, W. Zhang, M. Bastiani, A. M. Petrozza, L. M. Herz, M. B. Johnston, H. Lin, H. J. Snaith, *Mater. Horiz.* **2015**, *2*, 315.
[20] E. T. Hoke, D. J. Slotcavage, E. R. Dohner, A. R. Bowring, H. I. Karunadasa, M. D. McGehee, *Chem. Sci.* **2015**, *6*, 613.
[21] J. Kim, S.-H. Lee, J. H. Lee, K.-H. Hong, *J. Phys. Chem. Lett.* **2014**, *5*, 1312.
[22] Q. Wang, Y. Shao, H. Xie, L. Lyu, X. Liu, Y. Gao, J. Huang, *Appl. Phys. Lett.* **2014**, *105*, 163508.
[23] Y. Shao, Z. Xiao, C. Bi, Y. Yuan, J. Huang, *Nat. Commun.* **2014**, *5*, 5784.
[24] J. F. Verwey, *J. Phys. Chem. Solids* **1970**, *31*, 163.
[25] O. Malinkiewicz, A. Yella, Y. H. Lee, G. M. Espallargas, M. Graetzel, M. K. Nazeeruddin, H. J. Bolink, *Nat. Photonics* **2013**, *8*, 128.
[26] C. J. Brabec, A. Cravino, D. Meissner, N. S. Sariciftci, T. Fromherz, M. T. Rispens, J. C. Hummelen, *Adv. Funct. Mater.* **2001**, *11*, 374.
[27] C. Bi, Q. Wang, Y. Shao, Y. Yuan, Z. Xiao, J. Huang, *Nat. Commun.* **2015**, 6, 7747.
[28] F. Huang, Y. Dkhissi, W. Huang, M. Xiao, I. Benesperi, S. Rubanov, Y. Zhu, X. Lin, L. Jiang, Y. Zhou, A. Gray-Weale, J. Etheridge, C. R. McNeill, R. A. Caruso, U. Bach, L. Spiccia, Y.-B. Cheng, *Nano Energy* **2014**, *10*, 10.
[29] A. Baumann, K. Tvingstedt, M. C. Heiber, S. Väth, C. Momblona, H. J. Bolink, V. Dyakonov, *APL Mater.* **2014**, *2*, 081501.
[30] R. S. Sanchez, V. Gonzalez-Pedro, J.-W. Lee, N.-G. Park, Y. S. Kang, I. Mora-Sero, J. Bisquert, *J. Phys. Chem. Lett.* **2014**, *5*, 2357.
[31] J.-H. Heo, H. J. Han, D. Kim, T. Ahn, S. H. Im, *Energy Environ. Sci.* **2015**, *8*, 1602.